Laser remote sensing of the mean wind

I.N. Smalikho, V.A. Banakh, F. Kopp, and C. Werner

Institute of Atmospheric Optics, Siberian Branch of the Russian Academy of Sciences, Tomsk, Russia
DLR-Institute of Atmospheric Physics D-82230 Weßling, Germany

Received February 19, 2002

The representativeness and accuracy of laser Doppler anemometer (LDA) mean wind velocity measurements in the planetary boundary layer under different conditions of atmospheric stability and earth surface roughness is studied, both theoretically and experimentally, for two measurements techniques: 1) Velocity-Azimuth-Display (VAD) and 2) Doppler Beam Swinging (DBS). In many instances LDA measurements better represent true mean wind than traditional point measurements, because of measured spatial temporal averaging.

Introduction

Radar wind profilers measure the atmospheric wind profiles up to the stratosphere,[10] and laser Doppler systems are accepted to give excellent wind data in the same environment. Now wind lidar is becoming a standard tool for environmental studies purpose. To apply such a system one has to know how long one has to measure to get the same mean wind as that obtained with standard wind measuring devices. Doppler lidars measure the wind component along the line of sight, i.e., along the direction of transmitted laser radiation propagation. By scanning with an appropriate technique, the 3D wind vector can be measured.[5,9] Figure 1 shows the schematic of measurements.

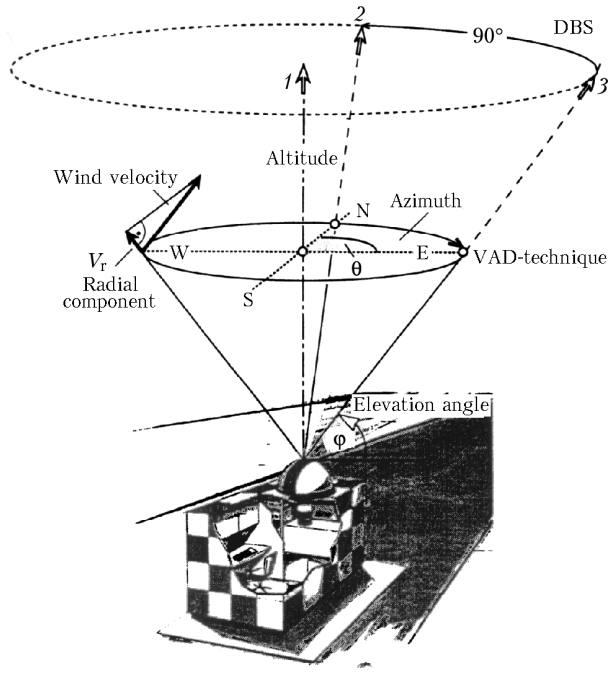

Fig. 1. Schematic of the measuring technique of a Doppler lidar (VAD scan or DBS technique).

A ground-based lidar with a scanner allows one to retrieve, in principle, the wind speed and direction throughout the entire troposphere. Necessary assumptions include homogeneity of the wind over the sensing volume. Turbulence has to be taken into consideration. This paper focuses on the question of how representative lidar wind measurements are in the boundary layer.

1. Doppler lidar

A frequency-stable, pulsed or continuous wave (cw) laser transmits energy with the frequency f_0 via a transmitting optics into the region of investigation in the atmosphere. The temporal pulse shape is either Gaussian (for a solid state laser) or like gain-switched spike (for the CO_2 laser). For the cw laser system – also called laser Doppler anemometer – the sensing volume can be defined by focusing in the layer (range) of investigation. Some of the radiation is backscattered by small aerosol particles which move with the prevailing wind speed across the laser focus volume.[9]

A line-of-sight (LOS) component of that wind is called radial component or V_r; it produces a Doppler shift Δf_D. This is obtained from the equation

$$\Delta f_D = 2 \frac{V_r}{c} f_0,$$

where c is the speed of light and f_0 is obtained from $f = c/\lambda$. At CO_2 laser wavelengths (λ) of 10.6 μm the velocity component of 1 m/s corresponds to a frequency shift, Δf_D, of 189 kHz.

By measuring at an azimuth angle θ and an elevation angle φ one gets a radial (line-of-sight) velocity V_r which depends on the wind vector components u, v, and w given by

$$V_r = u \sin\theta \cos\varphi + v \cos\theta \cos\varphi + w \sin\varphi.$$

The frequency shift can be measured in the backscattered signal, which is received with the receiving optics (same path as transmitting). A polarization switch is used to

0235-6880/02/08 607-08 $02.00

separate the outgoing radiation from the backscattered radiation. The backscattered radiation is mixed on a detector with the radiation of a local oscillator (LO) laser. A locking loop is used to keep the LO frequency and the transmitted laser frequency within a given bandwidth.

1.1. Velocity-Azimuth-Display (VAD) technique

To determine the magnitude and direction of the horizontal wind from measured LOS component, some type of scanning over azimuth and elevation angles is required.[5] Lhermitte and Atlas[13] showed that it is possible to retrieve mean horizontal wind magnitude and direction from radial velocity data acquired on the horizontal circles centered about the vertical axis of the scanner (Fig. 1). This type of the pattern is called a conical scan because the lidar beam sweeps a cone with the apex at the scanner. In an ideal case of a homogeneous atmosphere, the measured LOS components follow a sine-wave behavior (Fig. 2). In a turbulent atmosphere deviations from the sine-wave can occur. The representativeness of wind values derived from scans over parts of circle has been made in Ref. 5.

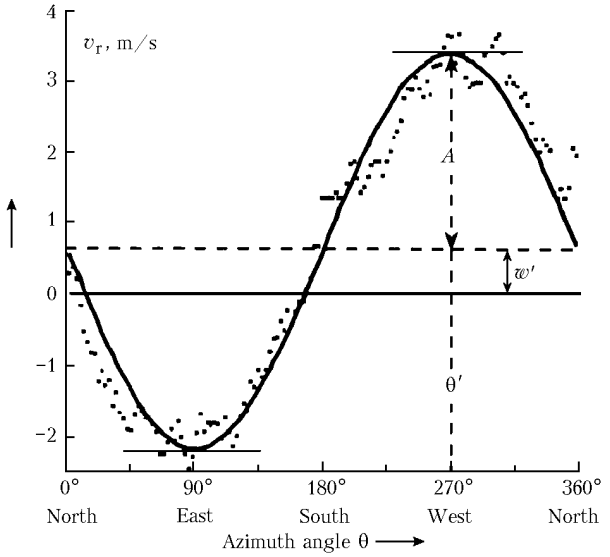

Fig. 2. Example of sine fitting of the radial wind velocity simulated with the use of the VAD technique.

With the meteorological definition of wind (speed, direction), one obtains

$$V_r = -u \sin\theta \cos\varphi - v \cos\theta \cos\varphi - w \sin\varphi, \quad (1)$$

where u is the West-East-wind component; v is the South-North-wind component; w is the vertical wind component; θ is the azimuth angle (clockwise from the North); φ is the elevation angle (see Fig. 1).

For the VAD scan for each range interval a separate "best" sine-wave fitting is necessary, yielding the offset w', the amplitude A, and the phase θ'. From these the following components are determined:

– wind direction θ' (Fig. 2),

– horizontal wind velocity v_{hor}

$$v_{hor} = \frac{A}{\cos\varphi} = \sqrt{u^2 + v^2}, \quad (2)$$

– vertical wind velocity w

$$w = -w'/\sin\varphi, \quad (3)$$

– horizontal wind components

$$u = \frac{A}{\cos\varphi} \sin\theta; \quad (4)$$

$$v = \frac{A}{\cos\varphi} \cos\theta. \quad (5)$$

1.2. Doppler Beam Swinging technique

For Doppler Beam Swinging (DBS) it is possible to measure wind components using only 3 beam-pointing directions (see Fig. 1). Here beam *1* points vertically, beam *2* to the North, and beam *3* to the East. With the convention, that $V_{r1} = w$, V_{r2} is the LOS component from North, and V_{r3} is the LOS component from East, the following relations are valid:

$$u = \frac{V_{r2} - V_{r1} \sin\varphi}{\cos\varphi}; \quad (6)$$

$$v = \frac{V_{r3} - V_{r1} \sin\varphi}{\cos\varphi}. \quad (7)$$

2. Turbulence effect assessment

Equation (1) is acceptable, when the velocity components u, v, and w are constant in time and space. Atmospheric wind turbulence causes fluctuations of the velocity V_r measured. That is, V_r is a random function of range R, direction (φ and θ), and time t. Temporal and spatial averaging of the wind velocity estimated from measured LOS components V_r allows one to acquire information about mean wind. In the case of measurement with a cw Doppler lidar in the atmospheric boundary layer, the turbulent fluctuations of V_r are the main source of the error in the mean wind estimate.

In the atmospheric boundary layer the statistical parameters of wind turbulence depend mainly on height, geostrophic wind, thermal stratification, and earth surface roughness. In this work we investigate the representativeness of laser Doppler anemometer (LDA) mean wind velocity measured by two techniques (VAD and DBS) in the planetary boundary layer under conditions of different atmospheric stability and earth surface roughness. The question to be addressed in this paper is: how many revolutions (VAD technique) should one use, and what duration of measurement (DBS technique) is necessary, to measure the mean wind with

a required accuracy? The mean wind normally is measured with a point sensor averaged over 10 minutes. As explained in Fig. 1, the LDA averages over a much large spatial volume than the point sensor. It is presumed that the measurement time for LDA is much smaller than 10 minutes (Ref. 1).

2.1. Theory

In the atmosphere the wind velocity vector $\mathbf{V}(\mathbf{r}, t) = \{V_z, V_x, V_y\} \equiv \{V_1, V_2, V_3\}$ is a random function of the coordinates $\mathbf{r} = \{z, x, y\} \equiv \{r_1, r_2, r_3\}$ and time t, where V_z, V_x, and V_y are, correspondingly, the vertical, longitudinal, and transverse components of instantaneous wind velocity. In what follows we assume that random variations of the wind velocity are caused by atmospheric turbulence only, that turbulent velocity field is statistically homogeneous and isotropic, and, that we can use the hypothesis of "frozen" turbulence:

$$\mathbf{V}(\mathbf{r}, t) = \mathbf{V}(\mathbf{r} + \langle \mathbf{V} \rangle t),$$

where $\langle \mathbf{V} \rangle = \{0, U, 0\}$, U is the mean wind velocity.

Let $\hat{\mathbf{V}} = \{\hat{V}_z, \hat{V}_x, \hat{V}_y\}$ be the wind velocity vector estimate obtained from measurement data. For an unbiased estimate $\langle \hat{\mathbf{V}} \rangle = \langle \mathbf{V} \rangle$ and $\langle \hat{V}_x \rangle = U$. Absolute and relative errors in the mean wind velocity measurement are $E = [\langle (\hat{V}_x - U)^2 \rangle]^{1/2}$ and $\varepsilon = E/U$, respectively. Later on we shall use ε_{PM}, ε_{VAD}, ε_{DBS} as relative and E_{PM}, E_{VAD}, E_{DBS} as absolute errors of mean wind velocity measurement with the point sensor (ε_{PM}, E_{PM}), and the cw Doppler lidar with scanning (VAD technique, ε_{VAD}, E_{VAD}), and with three beams (DBS technique, ε_{DBS}, E_{DBS}).

For a point velocity sensor the longitudinal component of wind velocity $\hat{V}_x$, averaged over time T, can be estimated as

$$\hat{V}_x = \frac{1}{T} \int_0^T \mathrm{d}t \; V_x(0, Ut, 0). \qquad (8)$$

The estimate (8) is unbiased ($\langle \hat{V}_x \rangle = U$). For the mean square error $\varepsilon^2_{\text{PM}}$ we have

$$\varepsilon^2_{\text{PM}} = \frac{2}{U^2 T^2} \int_0^T \mathrm{d}\tau \; (T - \tau) \; B_{22}(0, U\tau, 0), \qquad (9)$$

where $B_{ik}(\mathbf{p}) = \langle V'_i(\mathbf{r} + \mathbf{p}) \; V'_k(\mathbf{r}) \rangle$ is the correlation wind velocity tensor, $V'_i = V_i - \langle V_i \rangle$.

We use in Eq. (9) the von Karman model for the longitudinal correlation function of wind velocity fluctuations[7]:

$$B_V(p) = \int_0^\infty \mathrm{d}\kappa \; \Phi_V(\kappa) \cos(\kappa p), \qquad (10)$$

where $\Phi_V(\kappa) = \frac{2}{\pi} \frac{\sigma_V^2 \, L_V}{(1 + 1.8 L_V^2 \, \kappa^2)^{5/6}}$ is the velocity spectrum, $\sigma_V^2 = \langle (V_x - U)^2 \rangle$ is the velocity variance, and L_V is the integral scale of the velocity correlation (the outer scale of turbulence), and $p = |p|$. As a result we obtain

$$\varepsilon^2_{\text{PM}} = \frac{1}{U^2} \int_0^\infty \mathrm{d}\kappa \; \Phi_V(\kappa) \; \mathrm{sinc}^2 \left(\frac{\kappa U T}{2} \right). \qquad (11)$$

It follows from Eq. (11) that for short averaging period $T \ll L_V/U$

$$\varepsilon^2_{\text{PM}} \approx \int_0^\infty \mathrm{d}\kappa \; \Phi_V(\kappa)/U^2 = \sigma_V^2/U^2.$$

For long averaging period under condition $T \gg L_V/U$

$$\varepsilon^2_{\text{PM}} \approx (\pi \Phi_V(0)/U^2)/(UT) = (\sigma_V/U)^2 \; 2L_V/(UT),$$

therefore for $T \gg L_V/U$ the error ε_{PM} is less than σ_V/U.

The estimate of wind velocity $V_{\text{D}}(\theta, t) \equiv V_{\text{r}}$ measured with a cw Doppler lidar during time t at the azimuth angle θ can be derived as follows

$$V_{\text{D}}(\theta, t) = \int_0^\infty \mathrm{d}z' \; Q_{\text{s}}(z') \; \mathbf{V}(z'\mathbf{S}(\theta) + \langle \mathbf{V} \rangle t) \; \mathbf{S}(\theta), \qquad (12)$$

where

$$Q_{\text{s}}(z) = \{\pi k a_0^2 \, [(1 - z/R)^2 + (z/ka_0^2)^2]\}^{-1}$$

is the function characterizing the spatial resolution; here R is the range of sounding (focal range), a_0 is the initial beam radius,

$$k = 2\pi/\lambda; \; \mathbf{S}(\theta) = \{\sin\varphi, \cos\varphi \cos\theta, \cos\varphi \sin\theta\} \equiv$$

$$\equiv \{S_1(\theta), S_2(\theta), S_3(\theta)\}.$$

It follows from Eq. (12) that the spatial averaging of wind velocity fluctuations along the beam axis occurs. The averaging volume is positioned near the point $z' = R$ and has the longitudinal size $\Delta z = (\lambda/2) \times (R/a_0)^2$, if the condition $R \ll 2\pi a_0^2/\lambda$ is fulfilled.[1]

When the Velocity-Azimuth-Display technique is used, the azimuth angle θ is a function of time: $\theta = \omega_0 t$, where ω_0 is the speed of the laser beam rotation about vertical axis of the VAD cone. The VAD estimate of wind velocity vector $\hat{\mathbf{V}} = \{\hat{V}_z, \hat{V}_x, \hat{V}_y\}$ is determined by use of the expression[1]

$$\hat{\mathbf{V}} = \frac{1}{T}\int_0^T \mathrm{d}t\; V_\mathrm{D}(\omega_0 t,\, t)\; \mathbf{F}(t), \qquad (13)$$

where averaging time $T = (2\pi/\omega_0)N$, N is the number of rotations, and

$$\mathbf{F}(t) = \left\{ \frac{1}{\sin\varphi}, \frac{2\cos\omega_0 t}{\cos\varphi}, \frac{2\sin\omega_0 t}{\cos\varphi} \right\}.$$

Equations (12) and (13) allow one to write the following formula for the mean square error of the VAD estimate of the wind speed:

$$\varepsilon^2_\mathrm{VAD} = \frac{4}{U^2 T^2 \cos^2\varphi} \iint_0^T \mathrm{d}t_1\, \mathrm{d}t_2 \cos\omega_0 t_1 \cos\omega_0 t_2 \times$$

$$\times \iint_0^\infty \mathrm{d}z_1\, \mathrm{d}z_2\, Q_\mathrm{s}(z_1)\, Q_\mathrm{s}(z_2) \times$$

$$\times \sum_{i,k=1}^{3} S_i(\omega_0 t_1)\, S_k(\omega_0 t_2)\, B_{ik}(\mathbf{p}), \qquad (14)$$

where

$$\mathbf{p} = z_1\, \mathbf{S}(\omega_0\, t_1) - z_2\, \mathbf{S}(\omega_0\, t_2) + \langle \mathbf{V} \rangle\, (t_1 - t_2).$$

When the Doppler Beam Swinging technique with three sounding beams at the same elevation angle φ is used, the estimate of wind velocity vector is made based on the relationship

$$\hat{\mathbf{V}} = \frac{1}{T}\int_0^T \mathrm{d}t\; \mathbf{V}_\mathrm{D}(t)\; A, \qquad (15)$$

where

$$\mathbf{V}_\mathrm{D}(t) = \{V_\mathrm{D}(\theta_1,\, t),\; V_\mathrm{D}(\theta_2,\, t),\; V_\mathrm{D}(\theta_3,\, t)\},$$

θ_1, θ_2, θ_3 are the beam azimuth angles, $A = \{A_{mn}\}$ is the matrix with the elements:

$$A_{11} = a_{32},\; A_{12} = a_{13},\; A_{13} = a_{21},\; A_{21} = b_{32},\; A_{22} = b_{13},$$

$$A_{23} = b_{21},\; A_{31} = c_{32},\; A_{32} = c_{13},\; A_{33} = c_{21},$$

$$a_{ik} = (D\sin\varphi)^{-1} \sin(\theta_i - \theta_k),$$

$$b_{ik} = -\,(D\cos\varphi)^{-1} (\sin\theta_i - \sin\theta_k),$$

$$c_{ik} = (D\cos\varphi)^{-1} (\cos\theta_i - \cos\theta_k),$$

$$D = \sin(\theta_3 - \theta_2) + \sin(\theta_1 - \theta_3) + \sin(\theta_2 - \theta_1).$$

Substituting Eq. (12) into Eq. (15), for the mean square error of the DBS wind velocity estimate we obtain

$$\varepsilon^2_\mathrm{DBS} = \frac{2}{U^2 T^2} \int_0^T \mathrm{d}\tau\; (T - \tau) \iint_0^\infty \mathrm{d}z_1\, \mathrm{d}z_2\, Q_\mathrm{s}(z_1)\, Q_\mathrm{s}(z_2) \times$$

$$\times \sum_{i,k=1}^{3} b'_i b'_k \sum_{l,m=1}^{3} S_l(\theta_i)\, S_m(\theta_k)\, B_{lm}(\mathbf{p}), \qquad (16)$$

where

$$b'_1 = b_{32}, \quad b'_2 = b_{13}, \quad b'_3 = b_{21};$$

$$\mathbf{p} = z_1\, \mathbf{S}(\theta_i) - z_2\, \mathbf{S}(\theta_k) + \langle \mathbf{V} \rangle\, \tau.$$

The correlation tensor $B_{ik}(\mathbf{p})$ in Eq.(14) and $B_{ml}(\mathbf{p})$ in Eq. (16) is determined, in accordance with the assumption of isotropic turbulence, as

$$B_{ik}(\mathbf{p}) = B_V(p)\, \delta_{ik} + \frac{1}{2}\, p\, \frac{\mathrm{d}B_V(p)}{\mathrm{d}p} \left(\delta_{ik} - \frac{p_i\, p_k}{p^2} \right), \qquad (17)$$

where δ_{ik} is the Kronecker delta, and $B_V(p)$ is given by the von Karman model (10).

2.2. Calculations

To calculate the errors ε_PM, ε_VAD, and ε_DBS, parameters U, σ^2_V, and L_V are needed as functions of height h. These can be estimated using a theory of the boundary layer of the atmosphere, and they depend on the surface roughness parameter z_0, the geostrophic wind velocity G, the Coriolis parameter f, and the vertical turbulent flux of heat H. There are only few models of the height profiles $U(h)$, $\sigma^2_V(h)$, and $L_V(h)$ (Refs. 1–3, 6–8, and 12). In our calculations here we use simple models for these parameters,[1] that depend on Monin–Obukhov length $L = -\,U^2_*/(0.4g\, H/T_0\, \rho_0\, C_p)$, where U_* is the friction velocity, g is the acceleration due to gravity, C_p is the air heat capacity, T_0 is the mean temperature, and ρ_0 is the air density. The friction velocity U_* as a function of the parameters z_0, G, and H is calculated using the theory (Ref. 12).

In Fig. 3 we show the calculated data on the relative ε (ε_PM, ε_VAD, and ε_DBS) and absolute E (E_PM, E_VAD, and E_DBS) errors of estimation of the mean velocity, as they depend on the measurement time T, for the height $h = 50$ m in the surface layer of the atmosphere. The errors ε_VAD, E_VAD and ε_DBS, E_DBS are calculated for ranges $R = 70$ m (*a*), 150 m (*b*), 300 m (*c*), and 1000 m (*d*). In calculations of ε_DBS and E_DBS we set $\theta_1 = 0°$, $\theta_2 = 120°$, and $\theta_3 = 240°$. Figure 4 illustrates the range dependence of the relative and absolute errors of VAD and DBS techniques. It is seen from Figs. 3 and 4 that due to spatial averaging of velocity fluctuations the accuracy of Doppler lidar measurements of the mean velocity is higher than the accuracy of point sensor measurements. The VAD technique is more accurate than the DBS technique, due to additional spatial averaging over the scanning cone.

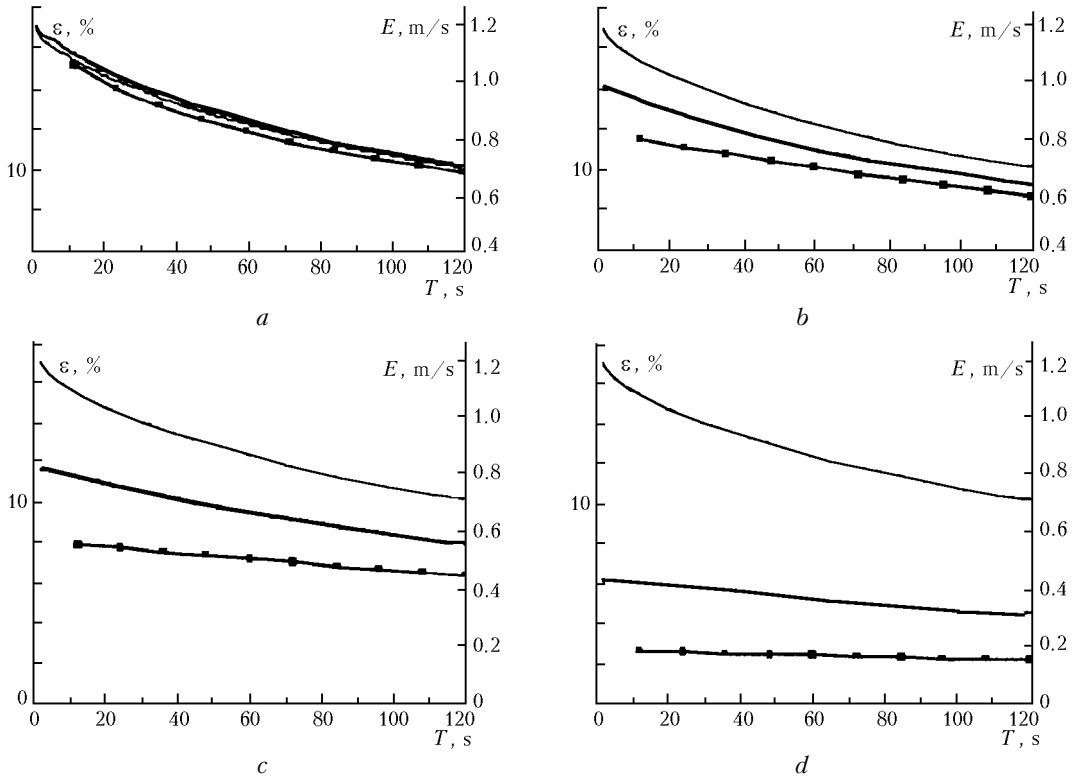

Fig. 3. Calculations of the time dependence of the relative and absolute errors of estimate of the mean wind velocity: ε_{PM}, E_{PM} (——); ε_{VAD}, E_{VAD} (—■—); ε_{DBS}, E_{DBS} (▬▬); $U = 7$ m/s, $\sigma_V = 1.2$ m/s, $L_V = 200$ m; $R = 70$ m, $\Delta z = 4.5$ m (*a*); $R = 150$ m, $\Delta z = 21$ m (*b*); $R = 300$ m, $\Delta z = 83$ m (*c*); $R = 1000$ m, $\Delta z = 920$ m (*d*); $h = 50$ m, $\varphi = \arcsin(h/R)$; $2\pi/\omega_0 = 12$ s.

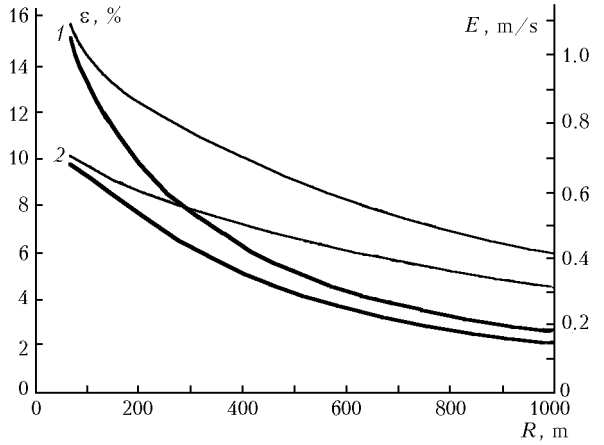

Fig. 4. Comparison of the range dependences of ε_{VAD}, E_{VAD} (▬) and ε_{DBS}, E_{DBS} (——) calculated for the measurement time $T = 12$ s (*1*) and 120 s (*2*). Parameters h, U, σ_V, L_V, and ω_0 are the same as in Fig. 3.

All calculations of the error in the mean wind velocity estimate for the heights exceeding 50 m have been carried out for the elevation angle of 30°. In Fig. 5 we show the height profiles of the errors ε_{PM}, E_{PM}; ε_{VAD}, E_{VAD} and ε_{DBS}, E_{DBS} calculated for different types of thermal stability of the atmospheric boundary layer. It is seen from the figure that in the case of unstable thermal stratification the averaging time 120 s is not sufficient to achieve $\varepsilon \le 10\%$ with the use of point wind sensor. At the same time in order to achieve the accuracy $\varepsilon < 10\%$ using the VAD technique, it is enough one rotation only, that is 12 s.

3. Measurements

Simultaneous measurements of the mean wind velocity by a cup anemometer, which can be considered as a point sensor, and by a scanning Doppler lidar were carried out by us earlier in 1992 in Lichtenau. The results of these experiments are published in Ref. 1. The comparison shows that the experimental values of ε_{PM} and ε_{VAD} obtained there are in a good agreement with the theoretical estimates made in section 2.2.

In order to compare the accuracy of the estimate of mean velocity by the VAD and DBS technique we have carried out the experiments on October 20 and November 4, 1999 in Oberpfaffenhofen. In the experiment we used a cw CO_2 Doppler lidar of the DLR Lidar Group. Beginning of the experiments (t_{start}) was at 15:40 local time on October 20 and at 9:40 on November 4. All measurements were made at the range $R = 150$ m and at the elevation angle $\varphi = 30°$, thus at 75 m height. We measured the radial velocity alternately at the fixed azimuth angles θ_1, θ_2, θ_3 and using the conical scanning with the laser beam about the vertical axis. Each measurement at a fixed azimuth angle θ_i took 21 seconds, each rotation took 7 seconds and we made 3 rotations. After that, we repeated the described procedure.

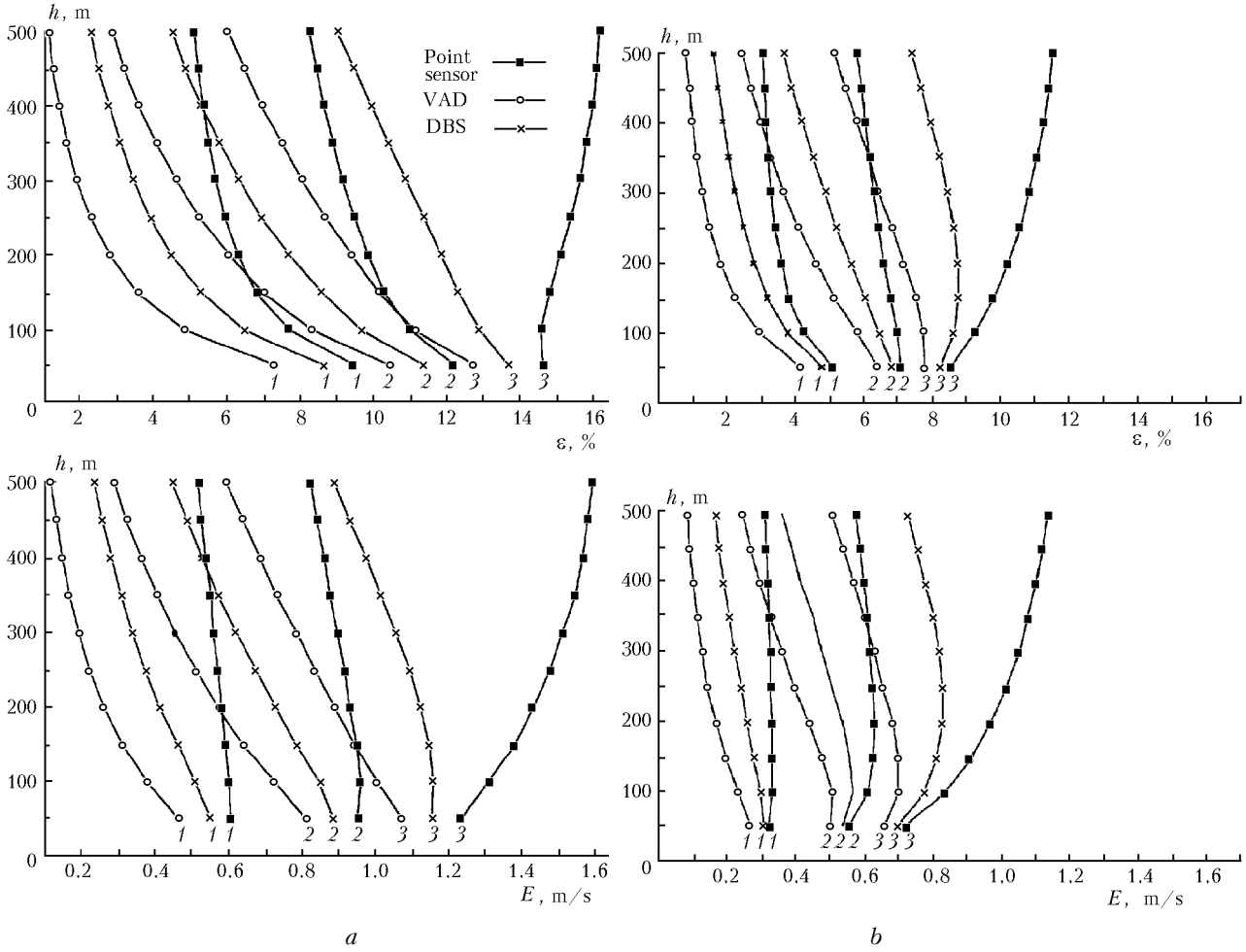

Fig. 5. Calculated height profiles of the relative ε_{PM}, ε_{VAD}, ε_{DBS} and absolute E_{PM}, E_{VAD}, E_{DBS} errors for the stable (curves *1*, $H = -20$ W/m^2), neutral (curves *2*, $H = 0$), and unstable (curves *3*, $H = 200$ W/m^2) stratifications. $z_0 = 10$ cm, $G = 10$ m/s, $\varphi = 30°$, $2\pi/\omega_0 = 12$ s, $T = 12$ (*a*) and 120 s (*b*).

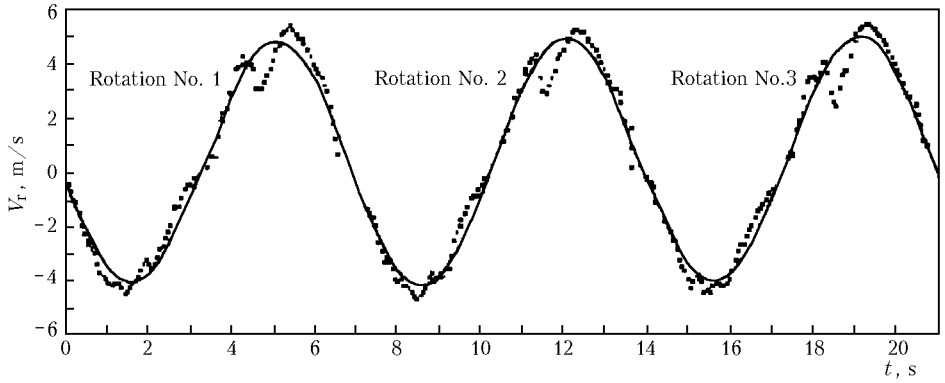

Fig. 6. Example of sine fitting of the radial wind velocity measured with the use of VAD technique. Measurements on 11.04.99.

In Fig. 6 we show an example of sine fitting (solid curve) of measured by the VAD technique radial velocity (points). The inhomogeneity of wind velocity is observed which persisted during all the three rotations.

Figure 7 demonstrates time behavior of the radial velocity measured by the DBS technique. The measurements were made at $\theta_1 = 98°$ ($t_{start} = 09{:}55$, beam No. 1), $\theta_2 = 222°$ ($t_{start} = 09{:}56$, beam No. 2), and $\theta_3 = 331°$ ($t_{start} = 09{:}57$, beam No. 3). At the bottom of this figure we show time behavior of the velocity components V_z, V_x, and V_y obtained from these estimates of the radial velocity under the assumption that measurements at the angles θ_1, θ_2, θ_3 were made simultaneously. It is seen that V_z estimate varies during measurement time in the

limits ± 1 m/s. Nevertheless, after time averaging of the data presented in Fig. 7 $\left(\hat{\mathbf{V}} = \frac{1}{T}\int_0^T \mathrm{d}t\ \mathbf{V}(t)\right)$ we have:

$\hat{\mathbf{V}}_z = 0.07$ m/s, $\hat{\mathbf{V}}_x = -4.18$ m/s, and $\hat{\mathbf{V}}_y = -0.16$ m/s.

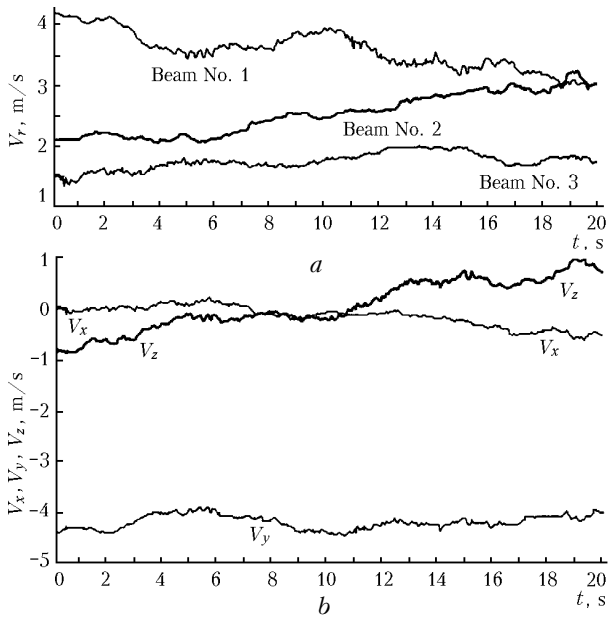

Fig. 7. Example of time behavior of the radial wind velocity and three components of the wind velocity measured with the use of the DBS technique. Measurements on 11.04.99.

In using the VAD technique the spatial averaging of the velocity fluctuations is greater than in the case of the DBS technique. However, the total time of one measurement by the DBS technique in these experiments is longer than that for a single revolution of the VAD technique by a factor of 3. Thus, we can expect that measurement accuracy of the mean velocity by both these methods should be approximately the same.

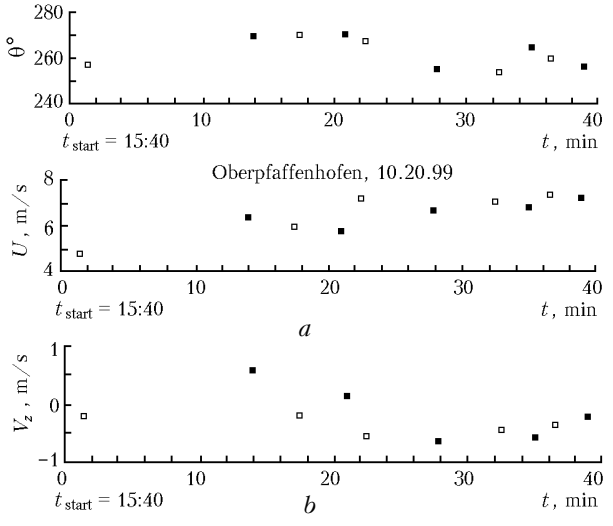

Fig. 8. Measurements on 10.20.99.

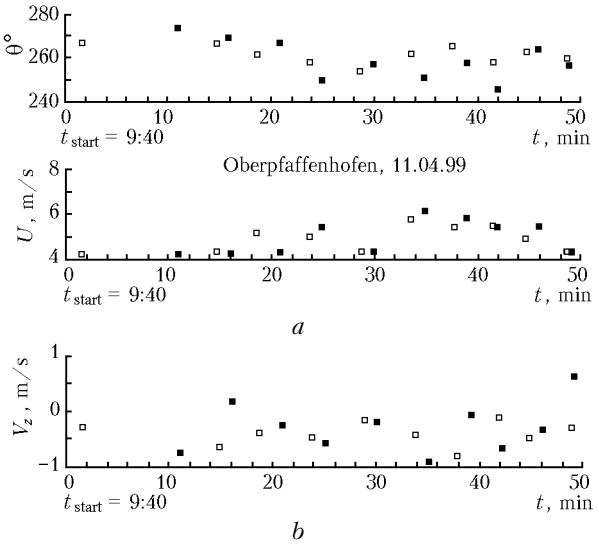

Fig. 9. Measurements on 11.04.99.

In Figs. 8 and 9 we present the measured results on the mean velocity, direction, and vertical component of the wind. Data of the VAD technique are shown by light squares and dark squares present data obtained using DBS technique. It is seen that both these methods give similar results. Variations of wind velocity components are caused by large-scale turbulent inhomogeneity of the wind and, possibly, by mesoscale processes in the atmosphere.

Conclusions

It follows from the above results that to obtain the mean wind by use of the sine-wave-fitting or the DBS technique for a given range resolution, one should measure and average data over a certain period. This period depends on system parameters like pulse repetition rate for a pulsed Doppler lidar or digitization rate for a cw Doppler lidar.

Let us assume that within 12 seconds there are enough data available for the VAD scan or the DBS technique. For example, with a 10-Hz pulse repetition rate, 120 data points could be acquired. It is useful to estimate the accuracy of the mean wind measurements for this fixed configuration depending on the surface roughness z_0, atmospheric stability, and range resolution.

Tables 1 to 3 contain the calculated measurement uncertainties, or errors, (relative and absolute) under given conditions.

Table 1. Measurement error depending on the surface roughness z_0 for neutral stability (H = 0). G = 10 m/s, Δz = 100 m, R = 250 m

Roughness z_0, cm	ε, %		E, m/s	
	VAD	DBS	VAD	DBS
0.1	2.6	6	0.23	0.53
1	3.5	7.9	0.3	0.67
5	4.4	9.9	0.36	0.8

Table 2. Measurement error depending on the atmospheric stratification. z_0 = 1 cm, G = 10 m/s, Δz = 100 m, R = 250 m

Stratification	ε, %		E, m/s	
	VAD	DBS	VAD	DBS
Stable (H = –40 W/m^2)	0.6	1.5	0.05	0.13
Neutral (H = 0)	3.5	7.9	0.3	0.67
Unstable (H = 400 W/m^2)	5.1	11.2	0.5	1.09

Table 3. Measurement error depending on the range resolution. z_0 = 1 cm, G = 10 m/s, neutral stability (H = 0)

Range resolution Δz, m	ε, %		E, m/s	
	VAD	DBS	VAD	DBS
100 (R = 250 m)	3.5	7.9	0.3	0.67
250 (R = 400 m)	2.3	5.9	0.2	0.5
1000 (R = 750 m)	1.2	3.3	0.1	0.28

From the tables one can see that for the cloud-free atmosphere one can estimate the mean wind profile within 12 seconds with the absolute accuracy of < 1 m/s, except under conditions of unstable stratification, using DBS technique (table 2). For poorer range resolutions (250 m for example) the 1 m/s is reached for all modeled cases in the turbulent boundary layer and above.

Acknowledgments

Support for the Institute of Atmospheric Optics in Tomsk was provided by the German Government, International Bureau. Project No. Ru–138 and by the Russian Foundation for Basic Research (Grant 00–05–64033).

References

1. V.A. Banakh, I.N. Smalikho, F. Kopp, and Ch. Werner, Appl. Opt. **34**, 2055–2067 (1995).
2. N.L.Byzova, B.N. Ivanov, and E. Garger, *Turbulence in the Atmospheric Boundary Layer* (Gidrometeoizdat, Leningrad, 1989), 263 pp.
3. B.G. Vager and E.D. Nadezhdina, *Atmospheric Boundary Layer under Conditions of a Horizontal Inhomogeneity* (Gidrometeoizdat, Leningrad, 1979), 192 pp.
4. F.F. Hall, Jr., R.M. Huffaker, R.M. Hardesty, M.E. Jackson, T.R. Lawrence, M.J. Post, R.A. Richter, and B.F. Weber, Appl. Opt. **23**, 2503 (1984).
5. R.L. Schwiesow, F. Kopp, and Ch. Werner. J. Atmos. Ocean. Technol. **2**, 3–14 (1985).
6. D.L. Laikhtman, *Physics of the Atmospheric Boundary Layer* (Gidrometeoizdat, Leningrad, 1961), 215 pp.
7. J.L. Lumley and H.A. Panofsky, *The Structure of Atmospheric Turbulence* (Interscience, New York, 1964), 263 pp.
8. A.S. Monin, and A.M. Yaglom, *Statistical Hydromechanics* (Nauka, Moscow, 1965, 1967), Part I and Part II, 683 pp.
9. M.J. Post and R.E. Cupp, Appl. Opt. **29**, 4145–4158 (1990).
10. H. Steinhagen, J. Dibbern, D. Engelbart, U. Görsdorf, V. Lehmann, J. Neisser, and J. Neuschaefer, Meteorolog. Zeitschrift, No. F.7, 248–261 (1998).
11. Ch. Werner, S. Rahm, S. Lehner, M. Buchhold, V. Banakh, and I. Smalikho, Pure and Appl. Opt. **7**, 1473–1487 (1998).
12. S.S. Zilitinkevich, *Dynamics of the Atmospheric Boundary Layer* (Gidrometeoizdat, Leningrad, 1970), 290 pp.
13. R.M. Lhermitte and D. Atlas, Amer. Met. Soc., 218–223 (1961).